Available online at www.sciencedirect.com
SCIENCE DIRECT
Solid State Communications 135 (2005) 765–768
solid state communications
www.elsevier.com/locate/ssc

Site-specific growth to control ZnO nanorods density and related field emission properties

C.C. Chang, C.S. Chang*

Department of Photonics and Institute of Electro-Optical Engineering, National Chiao-Tung University, 1001 Ta-Hsueh Road, Hsin-Chu 300, Taiwan, ROC

Received 28 March 2005; accepted 11 April 2005 by K.-A. Chao

Available online 22 April 2005

Abstract

Uniformly distributed ZnO nanorods with two different densities were demonstrated using the standard submicron semiconductor process. Plasma-enhanced chemical vapor deposition and UV-lithography were used to predefine growth sites and to grow ZnO nanorods at 600 °C. Integrated and local field emission (FE) experiments were also performed in the same substrate, and both involved the F–N vacuum tunneling mechanism. A medium density of high aspect ratio nanorods shows better FE performance due to the screening effect. The ability to control the growth-site demonstrated the possibility of the integration and the better field emission properties of nanodevices by ZnO on silicon substrate.

PACS: 79.60; 79.70

Keywords: A. ZnO nanorods; D. Density; D. F–N tunnel; D. Field emission; D. Site-specific

1. Introduction

Zinc oxide (ZnO) is one of the most promising oxide semiconductor materials. It can be used to make optoelectronic devices such as field-emission displays and diode lasers [1]. The field emission (FE) characteristics of ZnO for both randomly distributed nanowire arrays [2] and nanowires on single tungsten substrate [3] have been studied recently. The FE characteristics of unspecific-site ZnO nanowires with various densities have also been discussed. Nanorods of low density generally yield low emitted currents which resulting in the high turn-on field. However, the screening effects of high-density nanorods reduce field enhancement factor, which cause to consume more power. The density and morphology of nanorods must clearly be better controlled for future applications [4]. Hence, the ability to control the density and the growth-site to avoid screening effect is of interest.

The fabrication of uniformly distributed nanoscale structures has recently attracted much attention. The sample was made through a thermal process with catalyst, which named VLS process [5]. A general technique for preparing nanorods is by entailing labor upon the desired materials within the pores of a nanoporous membrane [6,7] or within the anodic alumina membranes (AAM) with ordered porous structures [8]. These two approaches can be used to predefine the placement of nanorods by locating metal catalyst islands or particles. However, the density and the distance between the pores and the size of pores in the template still restrict the growth pattern, besides the process is not compatible with the standard semiconductor process.

Many alternative methods for synthesizing nanosized arrays of rods, wires, fibrils and tubules have also been proposed at high temperatures [9,10]. The manufacturing microelectric process is usually conducted under relatively

* Corresponding author. Tel.: +886 3 5712171x56332; fax: +886 3 5716631.

E-mail address: cschang@mail.nctu.edu.tw (C.S. Chang).

0038-1098/$ - see front matter © 2005 Elsevier Ltd. All rights reserved.
doi:10.1016/j.ssc.2005.04.009

low temperature to avoid the phase transformation and atomic interdiffusion of device materials. Therefore, the site-specific nucleation of nanorods must occur along with a low-temperature growth process that remains different densities and is compatible with the device platform of interest [11]. However, very little work has been performed on the one-dimensional nanostructural system of ZnO formed using the submicron semiconductor process.

This work aims to demonstrate the site-specific growth to control density of ZnO nanorods on silicon substrate with standard submicron lithography process. Site-specific nanorods of ZnO were successfully grown at low temperature and the FE properties of those nanorods were also investigated. In addition, this technique also gives advantages of controlling the growth site and varying the proper interrod distance as well as the uniformly distributed emitter density while growing the ZnO nanorods.

2. Experiment

The site-specific substrate was made from a standard semiconductor process. First, 400 nm silicon dioxide was grown on a p-Si substrate by PECVD at 250 °C. Second, two different densities of array of 0.2 μm via holes were generated through submicron lithography and dry etching. Third, a thin Au layer was deposited on the substrate by RF sputtering and then silicon dioxide was partly removed by the lift-off process. Consequently, an Au dot, as a catalyst, was placed on the flat surface of every hole predefined by residual silicon dioxide.

The ZnO nanostructures were fabricated from Zn powder on the prepared patterning substrate by a thermal evaporation process in vacuum. The synthesis was carried out in a quartz tube with Zn powders as the source material. The temperature at the source position and the patterned substrate was set to 600 °C. During evaporation, Ar as a carrier gas flowed inside the quartz tube. After evaporation for 2 h, gray products were observed on the surface. The morphologies and microstructural properties of the products were investigated by field emission scanning electron microscopy (FESEM). Both integrated or the overall area FE and the local FE measurements were investigated. The former was made using two-parallel-plate configuration in a vacuum chamber. The cathode made by patterned nanorods of ZnO remained 100 μm away from the anode which is a large-area glass plate with phosphor-coated. As for the local FE properties, the anode was changed to a tip with radius of 600 μm to measure the different areas of different densities in the same sample. The separation was also fixed at 100 μm and the emission current was measured by a Keithley *I–V* meter. Contact currents could be distinguished from the FE current by a sudden current increase. The base pressure of the FE chamber was better than 10^{-5} Torr.

3. Results and discussion

Fig. 1(a) and (b) display images of high and medium densities of the site-specific growth of ZnO nanorods obtained by FESEM. Arrayed ZnO nanorods were grown from each 0.2 μm via hole. A wetting layer under these nanorods was found inside each hole, and the direction of the nanorods was changed according to the morphologies of that wetting layer. After decreasing the carrier gas, the number of ZnO nanorods in every hole was reduced. As shown in the more highly magnified image, a single nanorod was stand vertically in a hole and its appearance was changed from hexagonal prismatic at the top to cylindrical at the base. The average diameter and length of these nanorods were about 100–200 nm and ∼1 μm, respectively.

Fig. 2 illustrates the integrated field emission property of ZnO nanorod array grown on the p-Si substrate. The emission current–voltage characteristics were analyzed using the following Fowler–Nordheim (FN) equation

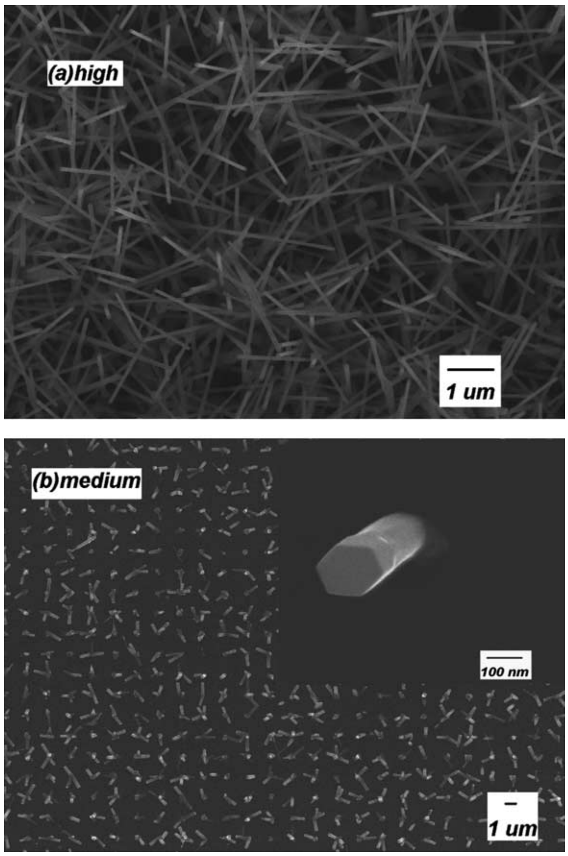

Fig. 1. (a) Patterned growth of high density ZnO nanorods. (b) Medium pattern density formed from each 0.2 μm via hole and the ZnO nanorod image of prismatic structure at the top part and cylindrical shape at the base part of the single ZnO nanorod.

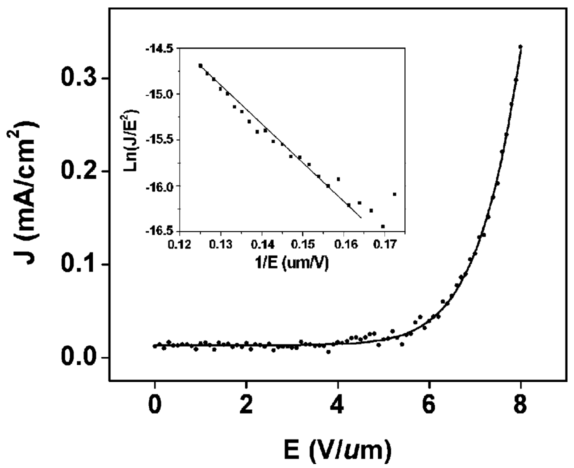

Fig. 2. The field emission *I–V* curves from the patterned ZnO nanorod array. The turn-on field was about 6.0 V/μm at current density of 0.05 mA/cm^2. The inset depicted F–N logarithmic plot, which satisfied the F–N tunneling mechanism by exhibiting a linear behavior over a measurement range.

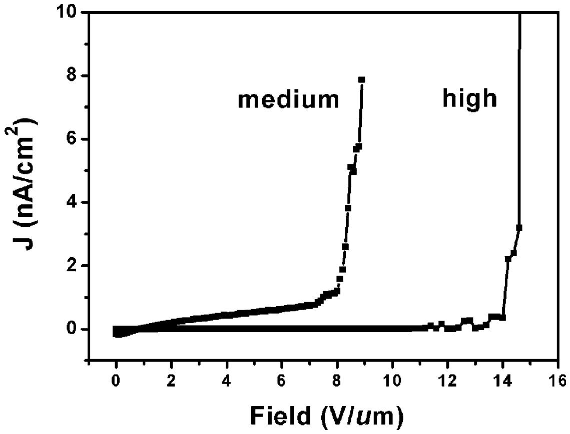

Fig. 3. The FE properties of different ZnO nanorod density. High density region show poor turn-on field about 14 V/μm, and the medium density area had better turn-on field about 8 V/μm.

$$J = A\left(\frac{\beta^2 V^2}{\phi d^2}\right)\exp\left(\frac{-B\phi^{3/2}d}{\beta V}\right) \tag{1}$$

where J is the current density; $A=1.56\times10^{-10}$ (AV^{-2} eV); $B=6.83\times10^9$ ($VeV^{-3/2}$ V/m); β is a field enhancement factor; ϕ is the work function; $E=(V/d)$ is the applied field; d is the distance between the anode and the cathode, and V is the applied voltage [12]. The turn-on field, which is defined as the field where the emission current density can be districted from the background noise, was approximately 6.0 V/μm at a current density of 0.05 mA/cm^2. The emission current density reached about 0.33 mA/cm^2 at an applied field of about 8.0 V/μm (the so-called threshold field) [2]. Both the turn-on and the threshold voltage were comparable to those of CNTs. Smaller or more sharply tipped nanorods, and a lower areal density of the nanorods yielded better FE properties which is similar to Jo et al. [4]. The emission current from ZnO nanorods produced sufficient brightness for flat panel displays [13]. Fig. 2 also presents the FN logarithmic plot, which exhibits linear behavior over the measurement range, so the emission is indeed caused by the F–N tunneling mechanism.

The local FE properties of different nanorods densities were shown in Fig. 3 and the average turn-on fields ($\sim$8 and 14 V/μm) were comparatively larger than that of the integrated FE property. The reason will be explained as follows. The integrated emission was dominated by a comparatively small number of very strong emitting sites spread out over the entire sample surface. Indeed, the number of detectable emission sites depends on the area of the measured surface. One square centimeter area will include more strong emitting sites, than a local measurement in 1 mm^2 window, hence a higher field enhancement factor (β) and a lower turn-on field is expected for integrated FE emission [14].

The poor emission of higher density nanorods is explained by an electrostatic screening effect provoked by the proximity of neighboring rods. The solution of the Poisson equation governs the behavior of the potential between the nearby ZnO deposit, hence β depends on the inter distance of nanorods (l). The β values, calculated from the FN logarithmic plot, of high and medium density of ZnO nanorods are and 443, 735 respectively. A function $f(l)=1-\exp(-1.1586l)$ that characterizes the decrease in the field amplification due to inter-rode screening [15]. Since it is the local electric field at the emission site that governs the emission, the distance between the nanorods remains a crucial parameter to optimize the FE. For the medium density, there is an ideal compromise between the emission current and the β factor, which shows a better FE performance.

4. Conclusions

In conclusion, ZnO nanorods were successfully grown on specific sites with a submicron semiconductor process at low temperature. A field emission experiment for such patterned ZnO nanorods was conducted to indicate the F–N tunneling model. Sample of medium density is shown a better field enhancement factor than that of higher density. Therefore, uniformly distributed the nanorods with a medium density by site-specific growth is thus clearly required and this approach was demonstrated the possibility of the integration of FE nanodevices by one-dimensional ZnO nanorods on a silicon substrate.

Acknowledgements

The authors would like to thank the National Science Council of the Republic of China for financially supporting this research under Contract No. NSC93-2112-M-009-027, and the Material Research Laboratories in the Industrial Technology Research Institute.

References

[1] E.A. Meulenkamp, J. Phys. Chem. B 102 (1998) 5566.
[2] Y.C. Kong, D.P. Yu, B. Zhang, W. Fang, S.Q Feng, Appl. Phys. Lett. 78 (2001) 407; M.H. Huang, Y.Y. Wu, H. Feick, N. Tran, E. Weber, P.D. Yang, Adv. Mater. 13 (2001) 113; C.J. Lee, T.J. Lee, S.C. Lyu, Y. Zhang, H. Ruh, H.J. Lee, Appl. Phys. Lett. 81 (2002) 3648.
[3] L. Dong, J. Jiao, D.W. Tuggle, J.M. Petty, S.A. Elliff, M. Coulter, Appl. Phys. Lett. 82 (2003) 1096.
[4] S.H. Jo, J.Y. Lao, Z.F. Ren, R.A. Farrer, T. Baldacchini, J.T. Fourkas, Appl. Phys. Lett. 83 (2003) 4821.
[5] C.C. Chang, C.S. Chang, Jpn. J. Appl. Phys. 43 (2004) 8360.
[6] C.R. Martin, Science 266 (1994) 1961.
[7] C.R. Martin, Chem. Mater. 8 (1996) 1739.
[8] H. Masuda, K. Fukuda, Science 268 (1995) 1466.
[9] M.H. Huang, S. Mao, H. Feick, H. Yan, Y. Wu, H. Kind, E. Weber, R. Russo, P. Yang, Science 292 (2001) 1897.
[10] Y. Li, G.W. Meng, L.D. Zhang, F. Phillipp, Appl. Phys. Lett. 76 (2000) 2011.
[11] Y.W. Heo, V. Varadarajan, M. Kaufman, K. Kim, D.P. Norton, F. Ren, P.H. Fleming, Appl. Phys. Lett. 81 (2002) 3046.
[12] H. Araki, T. Katayama, K. Yoshino, Appl. Phys. Lett. 79 (2001) 2636.
[13] Actually, 0.1 mA/cm^2 can produce enough brightness (.1000 cd/m^2) under practical display operating conditions
[14] L. Nilsson, O. Groening, C. Emmenegger, O. Kuettel, E. Schaller, L. Schlapbach, H. Kind, J.-M. Bonard, K. Kern, Appl. Phys. Lett. 76 (2000) 2071.
[15] J.M. Bonard, N. Weiss, H. Kind, T. Stockli, L. Forro, K. Kern, A. Chatelain, Adv. Mater. 13 (2001) 184.